Chapter 1

Overview: Molecular Electronics and Nanofluidics

1.1 Introductions: Recent Advances in Molecular Electronics

The field of molecular electronics is largely based on harnessing the power and versatility of chemical synthesis to control the properties of electronic devices and circuits. This field, which dates back several decades, has exploded in recent years. The reasons behind this are multifold. First, researchers have become increasingly adept at synthesizing molecules that are potentially interesting from the perspective of molecular electronics device properties. Second, rigorous surface science methods have been adapted for the task of quantitating the properties of the molecule/electrode interface. Third, continued scaling of electronics devices to nanometer dimensions has brought added incentive to this field. Fourth, a few theoretician are beginning to generate reliable and predictive models that go well beyond capturing 'model' systems but instead are beginning to yield real insight into more complex and realistic device properties. Finally, a host of new and unique device demonstrations that are enabled by both the molecules and the electronics platforms have been reported. For example, within recent years, molecular electronic switches (1, 2), light harvesting devices (3), molecular electronic based random access memory and configurable logic circuits (4), molecular mechanical biosensors (5), actuated molecular valves (6), ion channel mimics (7), molecular muscles (8-11), and novel electrochromic devices (12) have all been demonstrated, and in each of these demonstrations the molecules have played an active and critical role.

A key result that has emerged over the past year or two has been the ability to measure the properties of a particular molecular electronic solid state device, and then to utilize those measurements to optimize and improve the device through solution-phase chemical synthesis. In other words, for at least a few systems, a feedback loop that links the properties of molecular electronic devices to properties that can be optimized through chemical synthesis has been established.

This chapter consists of two major stories in different streams: the first and major story will be on molecular electronics, whereas the second and relatively minor story will be on nanofluidics. They are tied together, however, in that the nanofluidics story relies on technological and nanofabrication advances that were achieved in the arena of fabricating and testing ultra-high density molecular electronic circuitry.

For molecular electronics, I will cover a subset of the recent advances in this field including those from my research group. First, I will review molecular electronic devices in which the molecules constitute the active (and thus enabling) element within the devices. For any molecular electronic device, understanding and controlling the molecular electronic interface is a necessity, and this will be the second highlighted topic. The recent application of infrared and Raman spectroscopies towards interrogating molecular monolayers – even when they are sandwiched between two electrodes, has opened up a powerful window into understanding these interfaces. Finally, switching molecules that have been developed and characterized in the Heath/Stoddart groups will be focused. Not only will be fundamental background of the molecules such as the correlation of molecular structure with the switching mechanism be covered, but I will

also discuss how the physical environment of the molecular switch influences molecular mechanical switching mechanism.

In the nanofluidics, I will introduce a first generation device that is ultimately intended as a platform for protein discovery and identification. Preliminary results on model systems will be discussed.

1.2 The Molecule/Electrode Interfaces

To a great extent, the success of molecular electronics will depend on whether the molecule/electrode interface can be understood and designed to optimize the exploitation of the designed molecular properties. Several molecular electronics devices, including rectifiers and molecular switch tunnel junctions (MSTJs), consist of a molecular monolayer sandwiched between two electrodes – and so are called two-terminal (2T) devices. 2T devices are not only interface-rich devices, but they are also devices in which the molecules are not easily characterized since they reside at a buried interface.

Fabrication techniques for the preparation of two-terminal sandwich devices include the use of self-assembled monolayers (SAMs), usually on gold or platinum surfaces, Langmuir-Blodgett films on metal or silicon surfaces, and the covalent attachment of molecules onto SiO_2 or silicon surfaces. Deposition of the top electrode is potentially a process that can damage the molecules, and so a number of methods have been reported with the object of avoiding or minimizing such damage. Examples include the use of a mercury drop (13-16) or an STM tip as the top electrode. These methods, while clearly non-destructive, are also limited to single device demonstrations. More scaleable methods, such as electron-beam or sputtering deposition of the top electrode

materials, are more general but potentially more damaging. Ideally the deposited metal will adhere to, but not destroy or penetrate, the molecular film. In addition, the metal/molecular interface should not dominate charge transport through the junction. If it does dominate, then the molecular properties themselves are difficult to interrogate using charge transport methods.

This interface has historically been very difficult to study, and, until recently investigations were primarily limited to the use of X-ray photoelectron spectroscopy (XPS) (17). However, those studies are now complemented by surface-sensitive infrared and Raman spectroscopies, atomic force microscopy (AFM) and time of flight secondary ion mass spectroscopy (TOF-SIMS) (18-24).

Studies have shown that if a deposited metal does not chemically react with the molecular layer in some way, device failure can also occur through penetration of the metal through the monolayer (and thus cause device shorting). If the metal does chemically react, then that reaction can either destroy or protect the functional properties of the molecular monolayer. For cases in which the molecules are small and/or loosely packed on a surface, metal deposition can be irreversibly damaging to the monolayer. However, many research groups have shown that when the molecule/metal system is designed carefully, the desired molecular functionality can remain intact upon deposition of the top electrode. This has been achieved by incorporating a reactive or sacrificial molecular moiety, thereby “protecting” the desired functional groups. Examples include designing the interface that the molecules present to the deposited metals with functionalities that will react with and adhere to those metals, such as thiols with Au or

Al (25). For more reactive metals, such as Ti, bulky molecular groups at the interface can, via steric interactions, prevent the penetration of impinging metal atoms (1, 18).

Even if the deposited metals neither short the devices nor destroy the molecules, they can still strongly influence the measured device properties. McCreery and coworkers investigated the role of background O_2 during the formation of a Ti/molecule interface(26) and found that trace amounts of O_2 (5×10^{-7} Torr) can influence both the resistance and the rectifying characteristics of the junction.

For some devices, such as single- or few-molecule break junctions(27-33), both metal electrodes are effectively deposited prior to deposition of the molecular component. Such devices allow for an independent assessment of how the composition of the molecule/electrode interface can influence charge transport through the molecule. In certain cases those interfaces have been found to be rate limiting to charge transport, meaning that the molecule/electrode interface can dominate the measured charge transport characteristics(34, 35).

1. 3 Spectroscopy of Molecular Electronic Devices

Researchers have recently begun to quantitatively characterize these interfaces by correlating spectroscopic analysis of the devices with device transport measurements.

By choosing a molecule/electrode system that was amenable to study with Raman spectroscopy, Nowak and McCreery have done a series of experiments on carbon/nitroazobenzene (NAB)/titanium/gold devices (21, 36). They have studied both how the titanium/gold evaporated film affects the molecular structure of the devices and the changes in the molecular layer with varying Ti top electrode thickness, over time

(from < one hour to two weeks) and with applied voltages. Upon evaporation of Ti onto the molecular layer of NAB, XPS shows formation of a Ti-N bond (21) and Raman spectroscopy shows that the NO_2 Raman modes are decreased (indicating some reduction of the NAB), which partially recover over a period of several days.

Spectroscopic feedback on these devices is especially interesting when coupled with electrical transport measurements. Figure 1-1 is adapted from reference 36(36). Figure 1A shows the molecular structure of NAB. Figure 1-1B illustrates the affect that the Ti evaporation has on the Raman spectrum of NAB with varying Ti thicknesses (from 1 to 5 nm). The spectrum shows a steady decrease in the peaks at 1107 (phenyl-NO_2 stretch), 1340 (NO_2 stretch) and 1450 (N=N vibration) with increasing Ti thickness. Similar changes take place when the NAB is reduced in a spectroelectrochemical experiment, indicating that the Ti reduces the NAB as it evaporates. Figure 1-1C summarizes some of the electrical measurements. Only the Raman modes assigned to the azo stretches (1401 and 1450 cm^{-1}) show changes with applied voltage. The ratio of the peak intensities for the 1401 and 1450 cm^{-1} bands indicates the oxidation state of the NAB molecule. When +3 V (carbon relative to Ti/Au) is applied, the molecule is reoxidized. The authors are able to reverse the oxidation when the voltage polarity is reversed to –1V (up to three times). This groundbreaking study represents one of the most complete characterizations of molecules embedded within 2T devices.

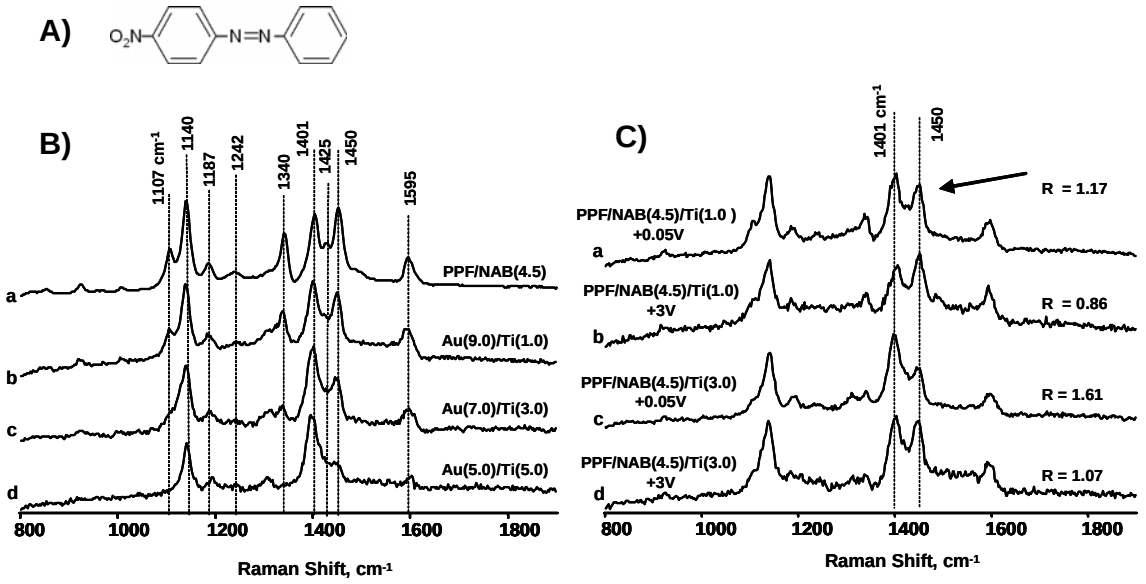

Figure 1-1. Raman spectrum of NAB with varying Ti thicknesses. (A) Structure of nitroazobenzene. (B) Raman spectra of PPF/NAB(4.5) surfaces before (a) and after (b-d) deposition of top contact. (C) Raman spectra of PPF/NAB(4.5) junctions with an applied bias voltage. Spectra b and d were acquired after a total of 270 s at +3 V(PPF relative to Ti). *R* is the ratio of peak intensities for the 1401 and 1450 cm^{-1} bands, measured relative to baseline. Reproduced with permission from reference 36. Copyright 2004 American Chemical Society.

Dr. DeIonno in my research group has investigated MSTJ devices, in which the molecular components are bistable, electrochemically switchable [2]catenanes or [2]rotaxanes(37). For these devices, spectroscopy on a device is not practical due to the very small cross-section of the active area (50 μm^2 to ~100 nm^2) and the choice of electrode materials. For a device that cannot be spectroscopically measured directly, spectroscopic measurements can be taken on a device analog and the current-voltage characteristics of the device can be correlated to the spectroscopic data. Dr. DeIonno performed a study on poly-Si/[2]rotaxane/Ti/Al crossbar MSTJs. The purpose of the

study was to determine the effect of transferring Langmuir monolayers at different pressures, and therefore different areas/molecule on device performance. Fourier transform reflection absorption infrared spectroscopy (FT-RAIRS) was used to determine the effect of Ti evaporation on the monolayers at the different pressures. The study showed that the transfer pressure of the monolayer affects both the FT-RAIRS and the transport properties. For lower transfer pressure, (i.e. larger area per molecule), the Ti metal evaporation affected a larger part of the molecule, leading to increased current and reduced switching performance in the devices.

1.4 Electrode Materials

Although metal has been the most commonly used electrode material, silicon has gained increasing interest due to existing infrastructure surrounding silicon-based devices, as well as the interesting material properties. Historically, my research group has fabricated the MSTJ devices using silicon (either poly-silicon or silicon-on-insulator (SOI), both passivated with the native oxide) (1), as the bottom electrode. These devices yield data that can be correlated back to the structure and physical properties of the molecule within the junction. Metal electrodes, by contrast (38), tend to yield molecule-independent device responses that originate from electrochemical processes or electromigration (filament formation) at the metal surface. More recently, there have been several in depth STM studies on silicon as an electrode material (39-44).

In collaboration with Lewis' group, my research group has studied a methyl-passivated silicon (111) surface with low temperature scanning tunneling microscopy (43). For this work, the Si(111) surface was initially chlorinated, and then alkylated using

the methyl Grignard reagent (45). This passivation yields a nearly atomically perfect surface, removing interface states (46) as well as stabilizing against oxidation. Several other groups have investigated silicon surfaces, typically with STM probes. For example, rectifying devices (47) as well as bistable switching of chemisorbed molecules (48) have been demonstrated.

Several interesting ultra high vacuum (UHV) STM studies have been done by Hersam group on silicon (100) surfaces. This surface, while more common to semiconductor manufacturing, does not yet have an accompanying chemistry that can render it stable to oxidation. Hersam and colleagues have studied a series of different molecules on both p-type and n-type Si(100). They have shown (and modeled using theory) negative differential resistance (NDR) signatures from several molecules (40-42). This work takes advantage of the silicon band edge to study the NDR effect. Depending on the silicon doping, NDR is seen at either positive (for p-type Si) or negative (for n-type Si) bias. In addition, they have studied the effect of packing density on transport and shown that for two molecules, cyclopentene and 2,2,6,6-tetramethyl-1-piperidinyloxyl (TEMPO), suppression of NDR occurs with increased packing density.

Another interesting result from the same group relates to the motion of individual organic molecules on the Si (100)-2 X 1 surface (49). They have shown that by using different molecules, they were able to predictably control molecular motion over the surface. Specifically, 4-methoxystyrene molecules were observed to translate laterally during STM imaging, while styrene molecules showed no detectable motion. They theorized that the additional rotational degree of freedom in the 4-methoxystyrene versus styrene was enabling the motion. They synthesized a third molecule, 5-vinyl-2,3-

dihydrobenzofuran, where the rotational degree of freedom is suppressed, which also led to the suppression of motion on the Si surface. These types of fundamental studies may eventually lend an additional degree of control over the behavior of molecules on surfaces.

1.5 Molecular Rectifiers

In 1974, Aviram and Ratner suggested the basic concept of molecular rectification. They proposed that a molecule, comprised of a donor-(σ-bridge)-acceptor sequence, could preferentially flow electrons in one direction(50), leading to asymmetric electronic transport. Based on this initial theory, many experimental groups have demonstrated molecular rectification (51-62) and have shown that modifications to the molecule can lead to changes in the rectification ratios, in a predictable way(51, 52, 56, 63).

A challenge in the fabrication of these devices is that rectification in a molecular electronic device is not always due to the molecular component. For example, it has been shown that in a junction (electrode/molecule/electrode), rectification can arise from the molecule/electrode interface (60, 61). Therefore, careful selection of the electrode material is critical. Oxidizable electrodes can give rise to a current-voltage asymmetry (18, 60-62, 64). In addition, asymmetric coupling of the molecular film to the electrodes can contribute to rectification, potentially masking or distorting the rectification from the molecule (60, 65).

Ashwell's group has demonstrated molecular rectification in a number of systems (51-58, 63). Critical to their work has been the both control experiments and careful selection of electrode materials. They prepared self-assembled monolayers of donor-(π-

bridge)-acceptor structures on gold substrates, which were probed by a Au or PtIr scanning tunneling microscope (STM) tip. The donor-(π-bridge)-acceptor structure was located in the center of the junction, by attaching the same length of alkyl chain to the STM tip and to the SAM on the substrate. In this way, they were able to exclude rectification effects from the molecule/electrode interface. Furthermore, they observed the reversible suppression of the rectification (51, 58) when donor-(π-bridge)-acceptor structure was chemically perturbed by HCl, which protonates the acceptor moiety. The rectification was restored when the device was exposed to NH_3.

More interestingly, the Ashwell's group (51, 52, 63) has also demonstrated the highest rectification ratio to date, ~450 at 1 V, from Au-S-$(CH_2)_3^-|A^+$-π-D structures (figure 1-2a). They first covalently attached 3-mercapto-1-propanesulfonate anion onto a gold substrate. Then, a *N*-methyl-5-(4-dibutylamino-benzylidene)-5,6,7,8-tetrahydroisoquinolinium cation (A^+-π-D) was aligned to the anion on the surface by self-organization. They attributed the very high rectification ratio to the fact that the ionic coupling allows one to maintain the polarity of the molecular structure more efficiently, as compared to LB films and SAMs of same dye molecule in which the iodide counter ion induces a dipole reversal, thereby reducing the rectification. In a similar study on the molecular rectification from LB films, my research group (59) demonstrated a rectification ratio of 18 at 0.9 V from a dye molecule of tetrathiafulvalene (TTF) donor-(σ-bridge)- tetracyanoquinodimeathane(TCNQ) acceptor. They attributed the rectification to the strong donor/acceptor character and this claim was supported by cyclic voltammogram (CV) data as well as molecular dynamic (MD) calculations. Even more

compelling is the fact that if the sequence of donor and acceptor moieties is reversed, the direction of rectification is also reversed.

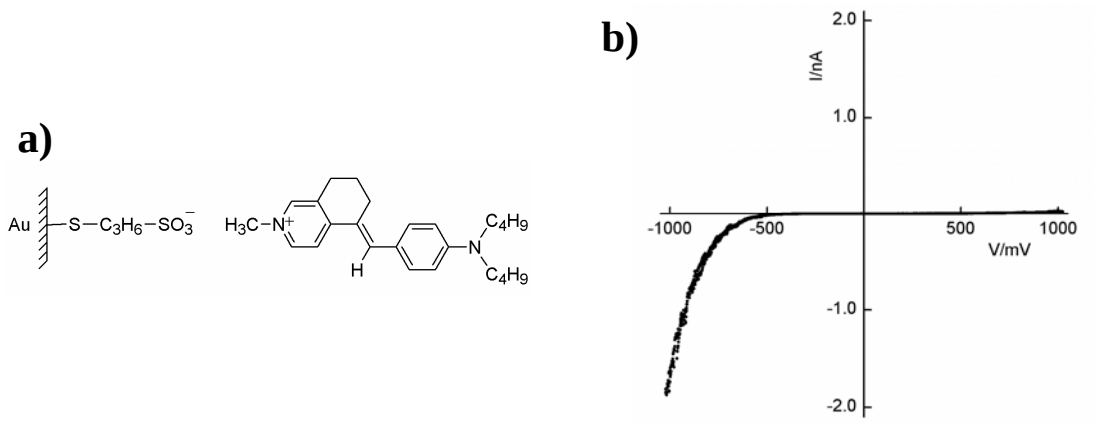

Figure 1-2. Molecular rectification from Au-S-$(CH_2)_3^-$|A^+-π-D structures. (a) Molecular structures of the chemisorbed 3-mercapto-1-propanesulfonate anion and ionically coupled *N*-methyl-5-(4-dibutylaminobenzylidene)-5,6,7,8-tetra-hydroisoquinolinium cation. (b) I–V characteristics from the molecule shown in (a) contacted by a PtIr probe. Data were obtained for a set point current of 0.1 nA and substrate voltage of –0.1 V and averaged for ten scans from the same site. The bias is designated by the sign of the substrate electrode. Reproduced with permission from reference 61. Copyright 2006 Royal Society of Chemistry.

1.6 Surface Immobilized Molecular Switches

Molecular electronic devices such as switches represent a more sophisticated molecular electronic device than rectifiers or resistors. This area has also advanced significantly over the past few years, with most work being carried out on bistable [2]rotaxanes, pseudorotaxanes, and [2]catenanes. These classes of switching molecule

have been studied mostly in two major platforms: immobilized on the surface by as self-assembled monolayers (SAMs) or using Langmuir-Blodgett (LB) technique and then embedded between two electrodes, thus mainly functioning as molecular switch tunnel junction (MSTJ) devices. Among these platforms, in this subchapter, I discuss the work on surface immobilized molecular switches accomplished by many groups in various applications.

Investigations of catenanes and rotaxanes prepared as molecular monolayers (Langmuir-Blodgett (LB)) films (66-68) or self-assembled monolayers (SAMs) (7, 66, 69), date back more than a decade, beginning with the early work of Lu, et al. in 1993 (70), with considerable amount of early work dedicated to the fabrication of these monolayers. More recent work has been focused on detecting and harnessing the molecular mechanical motions of bistable rotaxanes, pseudorotaxanes, and catenanes prepared as in LB films, SAMs, and other molecular monolayers. Recent works have shown that these molecular switches are controllable by appropriate chemical, electrochemical and optical stimuli.

Optically driven switching processes(3, 67, 70-72) have been demonstrated by several groups. Chia et al. (73) demonstrated the photochemically and chemically-induced reversible threading of pseudorotaxanes anchored onto a sol-gel surface, and found evidence for reversible threading that correlated well with similar measurements in the solution phase.

Electrochemically driven switching processes (74, 75) for different applications have also been demonstrated. Fitzmaurice's group has investigated both pseudorotaxanes (76) and bistable [2]rotaxanes (77) bound to the surfaces of TiO_2 nanoparticles. They

reported that a crown ether ring could be threaded onto the pseudorotaxane after the tripodal viologen was assembled onto the nanoparticle surface. For the case of the [2]rotaxane, it was also possible to electronically address and switch the bound rotaxane, through a process that involved transferring between one and four electrons from the conduction band of the TiO_2 nanoparticle to the viologen recognition sites. More recently, they developed a new NMR technique (78), paramagnetic suppression spectroscopy (PASSY), which allowed them to see structural conformation of these switching molecules at different redox states.

Other groups have utilized the electrochemical driven switching processes as molecular valves. Kim's group (7) has demonstrated chemically-induced reversible threading of a pseudorotaxane SAM on Au surface. A novel aspect of this work was that the threading/dethreading process could be utilized as a gate, allowing or preventing access of ions to the electrode surface. This striking result led the authors to make an analogy with how ion channel proteins gate ion transport in and out of cells. Hernandez, et al. (6) also covalently bonded pseudorotaxanes to the surface of a mesoporous material. Initially, the pores were diffusion-filled with a fluorophore, and then a $CBPQT^{4+}$ ring was threaded. Reduction of the $CBPQT^{4+}$ ring with $NaCNBH_3$ led to the dethreading of the rings from 1,5-dioxynapthalene (DNP) recognition site, which was followed by the release of the fluorophore.

Electrochemically driven switching processes have also been applied as biological sensors. Willner's group (5) has reported a rotaxane self-assembled onto an Au electrode. This molecule was utilized to shuttle charge between a redox-active enzyme and the surface (figure 1-3). In that work, the linear component of a pseudorotaxane

incorporating a diimine recognition site was assembled stepwise on the Au surface, threaded with a $CBPQT^{4+}$ ring, and then stoppered with flavin adenine dinucleotide (FAD). The FAD provides for a binding site for glucose oxidaze enzyme. They demonstrated that, under open circuit conditions, the oxidation of glucose leads to a reduction of the $CBPQT^{4+}$ ring on the rotaxane. This results in a translation of the ring to a position close to the electrode, where it is re-oxidized and then returns to the diimine recognition site. Thus, the $CBQT^{4+}$ ring acts as a charge shuttle between the Au electrode and the glucose oxidaze.

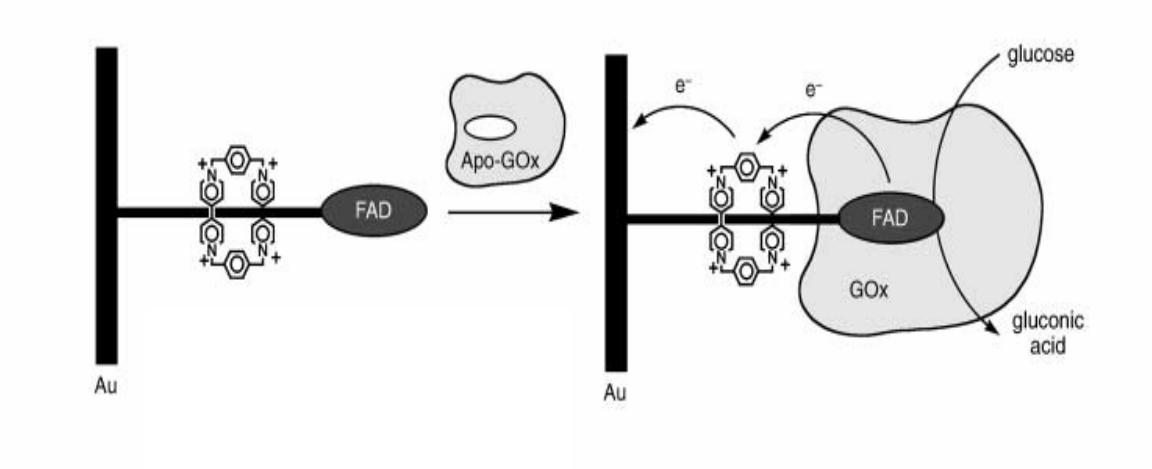

Figure 1-3. Molecular switching of pseudo-rotaxanes driven by biological reactions. Schematic representation of binding apo-GOx on pseudorotaxane-FAD self-assembled onto an Au and the mechanism of bioelectrocatalytic oxidation of glucose. Reproduced with permission from reference 5. Copyright 2004 Wiley-VCH Verlag GmbH.

1.7 Heath/Stoddart Switching Molecules: Basics and Directions

In the next platform, switching molecules embedded between top and bottom electrodes, Heath/Stoddart groups have made significant progresses into achieving a

better understanding of their switching mechanism within such confined environments including quite complex memory circuits, which require the integration of the switching molecules with a nanowire crossbar array.

In general, bistable [2]catenanes and [2]rotaxanes consist of two mechanically interlocked (or threaded) components. The two interlocked components are oriented with respect to one another in either of at least two conformations through non-bonding interactions. The detailed structures of those molecules are presented in figure 1-4. While studies for both [2]catenanes and [2]rotaxanes have been performed to almost identical extent, the major focus of my studies has been on a set on [2]rotaxanes. Therefore, [2]rotaxanes will lead the story in the following chapters.

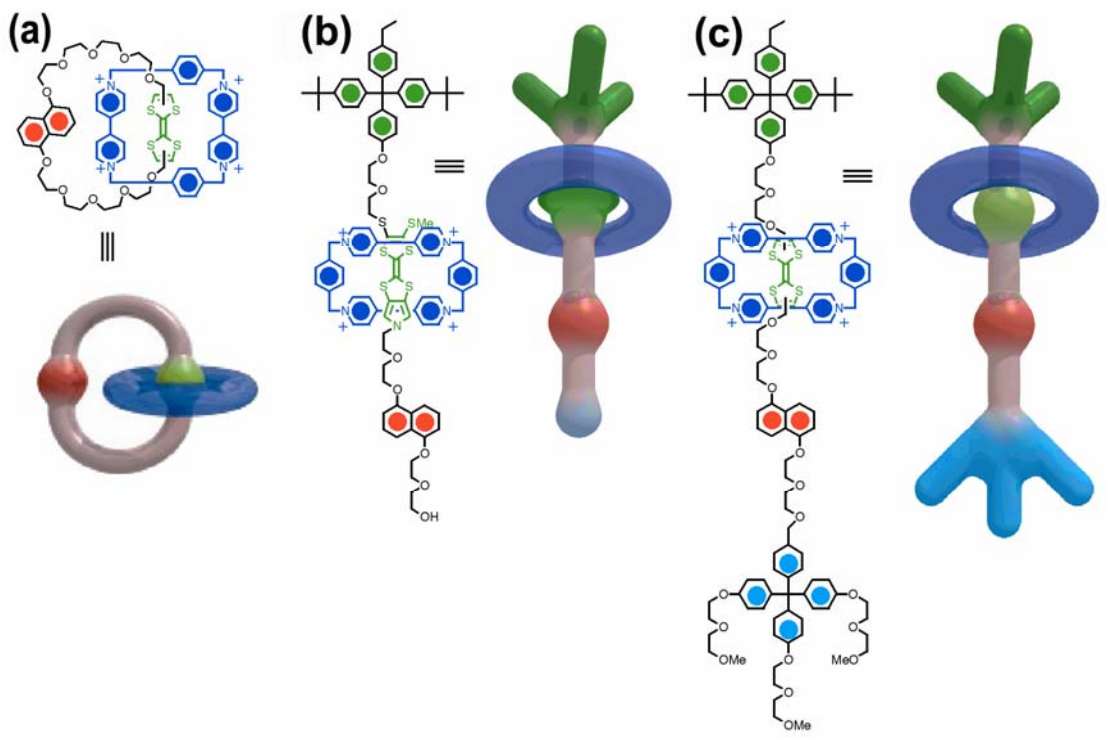

Figure 1-4. Bistable molecular mechanical switching molecules, each with similar recognition groups. (a) A [2]catenane, which is a molecular structure consisting of two

interlocked rings. A crown ether ringing containing tetrathiafulvalene (TTF) and dioxynapthalene (DNP) recognition units are threaded through a tetracationic cyclobisparaquat ($CBPQT^{4+}$) ring. (b) A pseudorotaxane containing a modified TTF unit, a DNP group on a thread component, and a $CBPQT^{4+}$ ring encircling the modified TTF unit. (c) A [2]rotaxane amphiphile, containing TTF and DNP units on a dumbbell component and a $CBPQT^{4+}$ ring. For each of these molecules, the lowest energy structure is shown ($CBPQT^{4+}$ ring) encircling the (modified)TTF unit. Many variations on these themes are possible, including molecular switches with modified recognition units, different ends on the dumbbell or thread components (for the [2]rotaxane and psuedorotaxane structures, respectively) for attaching the molecules to different surfaces, etc.

The advantage of these switching molecules is that they can be switched precisely by applying appropriate redox stimuli between two conformations (figure 1-5a). These two conformations are separated by an energy barrier. While an equilibrium exists between the two co-conformers, that equilibrium is typically shifted towards one (the ground-state co-conformation, or GSCC) and away from the other (the metastable-state co-conformation, or MSCC). One example is the bistable [2]rotaxane shown in figure 1-5a. In figure 1-5a, the $CBPQT^{4+}$ ring encircles a tetrathiafulvalene (TTF) unit on a dumbbell-shaped component, which represents the GSCC. The MSCC is the structure in which the $CBPQT^{4+}$ ring encircles the dioxynapthalene (DNP) unit. For this and related other molecules, a GSCC dominated distribution is switched to an MSCC dominated distribution via oxidation of the TTF unit ($TTF \rightarrow TTF^{+\cdot}$). The detailed switching cycle is shown in figure 1-5b.

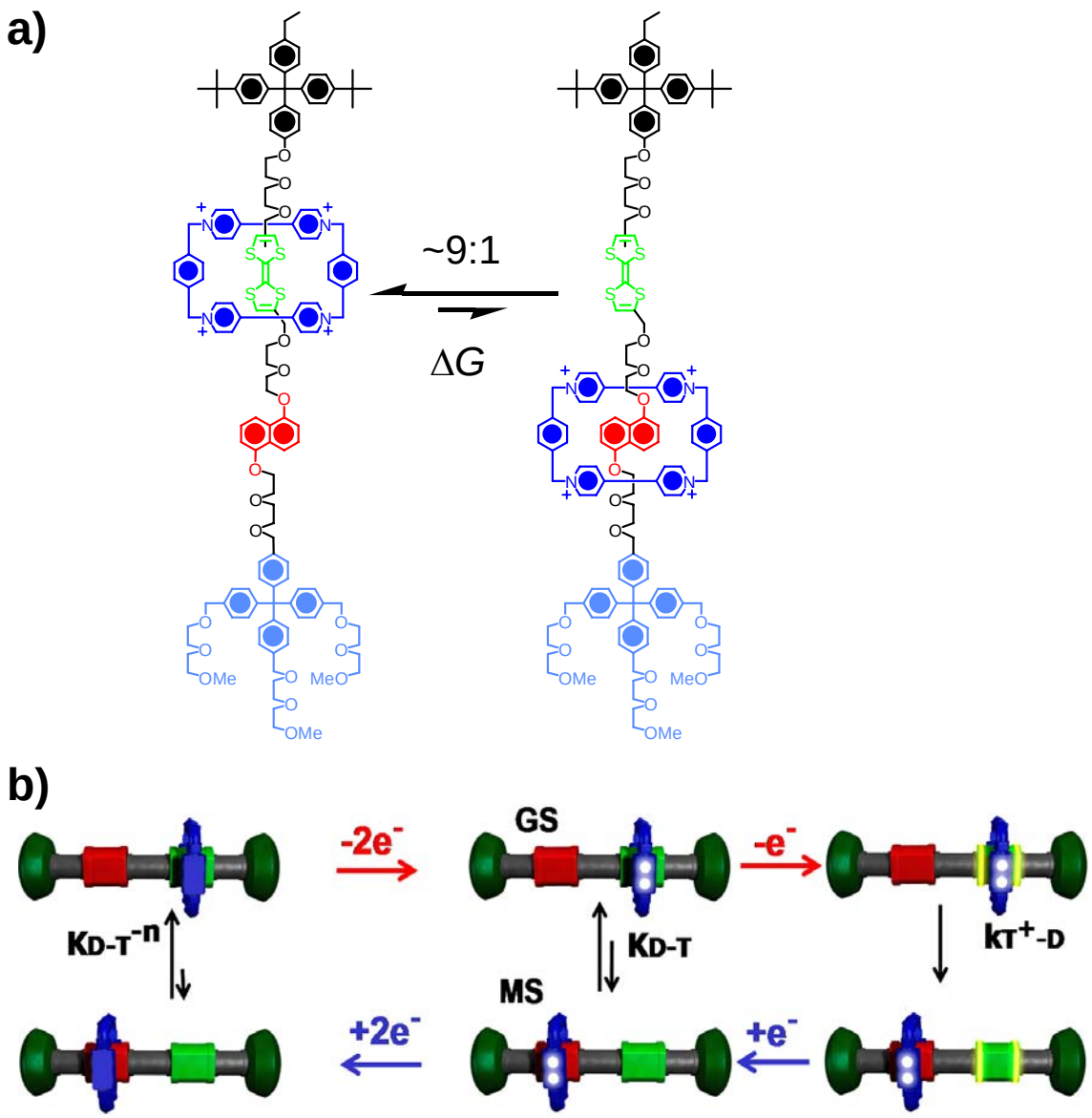

Figure 1-5. Molecular switching of bistable [2]rotaxanes. (a) Structural formulas of the two translational isomers of the representative bistable rotaxane corresponding to the ground state co-conformation (GSCC) and the metastable state co-conformation (MSCC). (b) The switching cycle for bistable [2]rotaxanes. The green and red sites on the dumbbell components correspond to tetrathiafulvalene (TTF) and dioxynapthyl (DNP) units, respectively. When the TTF unit is oxidized, it is drawn with highlighted green. The blue ring corresponds to the $CBPQT^{4+}$ ring carrying the positive charges indicated as

white spots. Reproduced with permission from reference 12. Copyright 2004 Wiley-VCH Verlag GmbH.

For the past several years, major efforts in my research group have been dedicated towards validate the switching mechanism especially as it applies to molecular electronic devices. The validation of the switching mechanism has been pursued in two directions. First, a number of these switching molecules have been tested in different physical environments including molecular switch tunnel junction (MSTJ) devices. Second, several [2]rotaxanes with different recognition units have been investigated in those physical environments. The overall objective has been to take fundamental molecular properties - the thermodynamic and kinetic parameters that describe the bistable switching mechanism - and attempt to understand how those properties are influenced by physical environment, including the environment of a molecular switch tunnel junction

Studies in different physical environments have demonstrated that this overall switching cycle is universal. However, $k_{D\rightarrow T,}$ a recovery rate from the MSCC to the GSCC-dominating equilibrium, exhibits a strong environmental dependence. As one moves from acetonitrile solution (79) to (high viscosity) polymer gels (12) to SAMs on Au surfaces (69) to a highly compressed LB monolayer sandwiched within an MSTJ(1, 4, 80-82), thermal decay corresponding to $k_{D\rightarrow T}$ in figure 1-5b is decreased by as much as 10^4-10^5.

The influence of the molecular structure on the ground-state equilibrium was also investigated in various environments (80). Two different [2]rotaxanes were tested: the [2]rotaxane shown in figure 1-5a and a rotaxane in which the TTF unit was replaced by a π-extended analogue (a bispyrrolotetrathiafulvalene, or BPTTF) (83). In contrast to the MSCC→GSCC relaxation kinetics, the thermodynamic equilibrium was found to be

relatively independent of environment, depending almost solely on molecular structure. In all environments, the TTF-based [2]rotaxane maintained a constant value (~9/1) of GSCC/MSCC equilibrium ($K_{(D/T)}^{4+}$) over broad range of temperatures, whereas BPTTF-based [2]rotaxane exhibited a strongly temperature-dependent GSCC/MSCC (1/1~3/1) over even smaller temperature range.

These studies in different environments not only validate the proposed switching mechanism, but provide evidence that one of the key device properties such as On/Off ratio is reflective of the molecular structure.

1.8 Scale-down: 160 kbit Molecular Electronic Memory Circuits

One of the major advantages of molecular electronics is a potential scaling of devices to molecular dimensions. In other words, until patterning techniques defining electrodes in the molecular dimensions are developed, the efforts to understand molecular electronics and how it might be applied to ultra-small devices would be academic.

For these reasons, my research group has developed a technique for the preparation of ultra-dense nanowire arrays, called the superlattice nanowire pattern transfer (SNAP) method. At the same time, through our collaboration with the Stoddart group, a variety of [2]rotaxanes have been developed and found to maintain somewhat robust switching characteristics within the MSTJs. Finally, ultra-dense molecular electronic crossbar circuits (84) were achieved by integrating the SNAP nanowires with optimized functional [2]rotaxanes (85). These memory circuits represent a world-record in terms of the bit density per unit area of an electronically addressable memory. They

were demonstrated to be capable of storing information and to function as complete circuits.

Consequently, the successful demonstration of these delicate circuits indicates that new materials and architectures based on nanotechnology could provide solutions to scale-down issues that have been very difficult to address with the current CMOS technology.

1.9 Nanofluidics

Owing to recent advances in fabrication technology, one could routinely generate nanostructures such as nanopores, nanowires and nanotubes. In particular, the capability of controlling geometry in one dimensional nanostructures has opened up a new field, nanofluidics.

The most noticeable character of the nanofluidics, compared to microfluidics, is small channel dimensions that are comparable to the size of macromolecules and are also comparable to the length scales associated with surface-charge Debye screening. The small channel dimensions bring many novel scientific phenomena as well as useful findings for applications. Entangled molecules could be stretched out along one dimension. This allow for specific chemical sites that are not readily accessible within the entangled molecule to be interrogated. A good example is the restriction mapping for DNA molecules(86). Also, the target molecules delivered to the nanochannel experience electrostatic interactions with the nanochannel walls because at least one dimension of the channel dimensions might be on the order of the Debye screening length. Under this condition, ionic transport would be dominated by the nanochannel surface charges and

charges carried by the ions(87, 88). This extraordinary feature can be utilized for biosensors(89). Moreover, extremely fast fluid flow is possible because no-slip condition may not hold true in several nanometer channel diameters(90-92).

1.10 Structure and Scope of the Thesis

The thesis is composed of four chapters. Each chapter has its own introduction, figures and references. Chapter 2 covers the kinetic and thermodynamic studies for bistable [2]rotaxanes. These studies were critical for validating the switching mechanism for [2]rotaxanes and [2]catenanes that had been previously proposed for their operation within molecular switch tunnel junction devices. Thus, all the claims and descriptions in chapter 2 now provide a foundation for the further understanding and development of these molecules within solid-state device settings. Chapter 3 is dedicated to the project of fabricating and testing the 160 kbit molecular electronic memory circuits. Completion of this project represented a long term goal of my research group - the production of fully functional molecular electronic memory devices at true molecular dimensions. This project required the development of non-trivial nanofabrication processes, and certain of those are presented in some detail. This chapter is also related to the results of chapter 2, since the successful demonstration of the operation of this memory circuit relies on the mechanistic models for the switching molecules that are covered in chapter 2. Chapter 4 covers the nanofluidics project. This project was initiated in the summer of 2006 and thus is currently in the early development stage, although there has been a significant progress. Future directions for this project are also described.

1.11 References

1. Collier, C. P., Mattersteig, G., Wong, E. W., Luo, Y., Beverly, K., Sampaio, J., Raymo, F. M., Stoddart, J. F. & Heath, J. R. (2000) *Science* 289, 1172-1175.
2. Pease, A. R., Jeppesen, J. O., Stoddart, J. F., Luo, Y., Collier, C. P. & Heath, J. R. (2001) *Acc. Chem. Res.* 34, 433-444.
3. Sheeney-Haj-Ichia, L. & Willner, I. (2002) *J. Phys. Chem. B* 106, 13094-13097.
4. Luo, Y., Collier, C. P., Jeppesen, J. O., Nielsen, K. A., Delonno, E., Ho, G., Perkins, J., Tseng, H. R., Yamamoto, T., Stoddart, J. F. & Heath, J. R. (2002) *Chemphyschem* 3, 519-525.
5. Katz, E., Sheeney-Haj-Ichia, L. & Willner, I. (2004) *Angew. Chem. Int. Ed.* 43, 3292-3300.
6. Hernandez, R., Tseng, H. R., Wong, J. W., Stoddart, J. F. & Zink, J. I. (2004) *J. Am. Chem. Soc.* 126, 3370-3371.
7. Kim, K., Jeon, W. S., Kang, J. K., Lee, J. W., Jon, S. Y., Kim, T. & Kim, K. (2003) *Angew. Chem. Int. Ed.* 42, 2293-2296.
8. Jimenez, M. C., Dietrich-Buchecker, C. & Sauvage, J. P. (2000) *Angew. Chem. Int. Ed.* 39, 3284-3287.
9. Jimenez-Molero, M. C., Dietrich-Buchecker, C. & Sauvage, J. P. (2003) *Chem. Com.*, 1613-1616.
10. Marsella, M. J. & Reid, R. J. (1999) *Macromolecules* 32, 5982-5984.
11. Taylor, E. W. (1993) *Science* 261, 35-36.

12. Steuerman, D. W., Tseng, H. R., Peters, A. J., Flood, A. H., Jeppesen, J. O., Nielsen, K. A., Stoddart, J. F. & Heath, J. R. (2004) *Angew. Chem. Int. Ed.* 43, 6486-6491.

13. Grave, C., Tran, E., Samori, P., Whitesides, G. M. & Rampi, M. A. (2004) *Synthetic Metals* 147, 11-18.

14. Slowinski, K., Fong, H. K. Y. & Majda, M. (1999) *J. Am. Chem. Soc.* 121, 7257-7261.

15. Tran, E., Rampi, M. A. & Whitesides, G. M. (2004) *Angew. Chem. Int. Ed.* 43, 3835-3839.

16. York, R. L. & Slowinski, K. (2003) *J. Electroanal. Chem.* 550, 327-336.

17. Konstadinidis, K., Zhang, P., Opila, R. L. & Allara, D. L. (1995) *Surface Science* 338, 300-312.

18. Chang, S. C., Li, Z. Y., Lau, C. N., Larade, B. & Williams, R. S. (2003) *Appl. Phys. Lett.* 83, 3198-3200.

19. Fisher, G. L., Hooper, A. E., Opila, R. L., Allara, D. L. & Winograd, N. (2000) *J. Phys. Chem. B* 104, 3267-3273.

20. Hooper, A., Fisher, G. L., Konstadinidis, K., Jung, D., Nguyen, H., Opila, R., Collins, R. W., Winograd, N. & Allara, D. L. (1999) *J. Am. Chem. Soc.* 121, 8052-8064.

21. Nowak, A. M. & McCreery, R. L. (2004) *Anal. Chem.* 76, 1089-1097.

22. Tighe, T. B., Daniel, T. A., Zhu, Z. H., Uppili, S., Winograd, N. & Allara, D. L. (2005) *J. Phys. Chem. B* 109, 21006-21014.

23. Walker, A. V., Tighe, T. B., Cabarcos, O. M., Reinard, M. D., Haynie, B. C., Uppili, S., Winograd, N. & Allara, D. L. (2004) *J. Am. Chem. Soc.* 126, 3954-3963.

24. Walker, A. V., Tighe, T. B., Stapleton, J., Haynie, B. C., Upilli, S., Allara, D. L. & Winograd, N. (2004) *Appl. Phys. Lett.* 84, 4008-4010.

25. de Boer, B., Frank, M. M., Chabal, Y. J., Jiang, W. R., Garfunkel, E. & Bao, Z. (2004) *Langmuir* 20, 1539-1542.

26. McGovern, W. R., Anariba, F. & McCreery, R. L. (2005) *J. Electrochem. Soc.* 152, E176-E183.

27. Liang, W. J., Shores, M. P., Bockrath, M., Long, J. R. & Park, H. (2002) *Nature* 417, 725-729.

28. Park, H., Lim, A. K. L., Alivisatos, A. P., Park, J. & McEuen, P. L. (1999) *Appl. Phys. Lett.* 75, 301-303.

29. Park, H., Park, J., Lim, A. K. L., Anderson, E. H., Alivisatos, A. P. & McEuen, P. L. (2000) *Nature* 407, 57-60.

30. Park, J., Pasupathy, A. N., Goldsmith, J. I., Chang, C., Yaish, Y., Petta, J. R., Rinkoski, M., Sethna, J. P., Abruna, H. D., McEuen, P. L. & Ralph, D. C. (2002) *Nature* 417, 722-725.

31. Reed, M. A., Zhou, C., Muller, C. J., Burgin, T. P. & Tour, J. M. (1997) *Science* 278, 252-254.

32. Reichert, J., Ochs, R., Beckmann, D., Weber, H. B., Mayor, M. & von Lohneysen, H. (2002) *Phys. Rev. Lett.* 88.

33. Xu, B. Q. & Tao, N. J. J. (2003) *Science* 301, 1221-1223.

34. Yaliraki, S. N. & Ratner, M. A. (1998) *J. Chem. Phys.* 109, 5036-5043.

35. Yu, H. B., Luo, Y., Beverly, K., Stoddart, J. F., Tseng, H. R. & Heath, J. R. (2003) *Angew. Chem. Int. Ed.* 42, 5706-5711.

36. Nowak, A. M. & McCreery, R. L. (2004) *J. Am. Chem. Soc.* 126, 16621-16631.

37. DeIonno, E., Tseng, H. R., Harvey, D. D., Stoddart, J. F. & Heath, J. R. (2006) *J. Phys. Chem. B* 110, 7609-7612.

38. Stewart, D. R., Ohlberg, D. A. A., Beck, P. A., Chen, Y., Williams, R. S., Jeppesen, J. O., Nielsen, K. A. & Stoddart, J. F. (2004) *Nano Lett.* 4, 133-136.

39. Cao, P. G., Yu, H. B. & Heath, J. R. (2006) *J. Phys. Chem. B* 110, 23615-23618.

40. Guisinger, N. P., Basu, R., Greene, M. E., Baluch, A. S. & Hersam, M. C. (2004) *Nanotechnology* 15, S452-S458.

41. Guisinger, N. P., Greene, M. E., Basu, R., Baluch, A. S. & Hersam, M. C. (2004) *Nano Lett.* 4, 55-59.

42. Guisinger, N. P., Yoder, N. L. & Hersam, M. C. (2005) *Proc. Nat. Acad. Sci.* 102, 8838-8843.

43. Yu, H. B., Webb, L. J., Ries, R. S., Solares, S. D., Goddard, W. A., Heath, J. R. & Lewis, N. S. (2005) *J. Phys. Chem. B* 109, 671-674.

44. Yu, H. B., Webb, L. J., Solares, S. D., Cao, P. G., Goddard, W. A., Heath, J. R. & Lewis, N. S. (2006) *J. Phys. Chem. B* 110, 23898-23903.

45. Bansal, A., Li, X. L., Lauermann, I., Lewis, N. S., Yi, S. I. & Weinberg, W. H. (1996) *J. Am. Chem. Soc.* 118, 7225-7226.

46. Royea, W. J., Michalak, D. J. & Lewis, N. S. (2000) *Appl. Phys. Lett.* 77, 2566-2568.

47. Lenfant, S., Krzeminski, C., Delerue, C., Allan, G. & Vuillaume, D. (2003) *Nano Lett.* 3, 741-746.

48. Mayne, A. J., Lastapis, M., Baffou, G., Soukiassian, L., Comtet, G., Hellner, L. & Dujardin, G. (2004) *Phys. Rev. B* 69, 045409.

49. Basu, R., Tovar, J. D. & Hersam, M. C. (2005) *J. Vac. Sci & Tech. B* 23, 1785-1789.

50. Aviram, A. & Ratner, M. A. (1974) *Chem. Phys. Lett.* 29, 277-283.

51. Ashwell, G. J., Chwialkowska, A. & High, L. R. H. (2004) *J. Mat. Chem.* 14, 2848-2851.

52. Ashwell, G. J., Ewington, J. & Moczko, K. (2005) *J. Mat. Chem.* 15, 1154-1159.

53. Ashwell, G. J. & Gandolfo, D. S. (2002) *J. Mat. Chem.* 12, 411-415.

54. Ashwell, G. J., Gandolfo, D. S. & Hamilton, R. (2002) *J. Mat. Chem.* 12, 416-420.

55. Ashwell, G. J., Hamilton, R. & High, L. R. H. (2003) *J. Mat. Chem.* 13, 1501-1503.

56. Ashwell, G. J., Mohib, A. & Miller, J. R. (2005) *J. Mat. Chem.* 15, 1160-1166.

57. Ashwell, G. J., Sambles, J. R., Martin, A. S., Parker, W. G. & Szablewski, M. (1990) *J. Chem. Soc. Comm.*, 1374-1376.

58. Ashwell, G. J., Tyrrell, W. D. & Whittam, A. J. (2003) *J. Mat. Chem.* 13, 2855-2857.

59. Ho, G., Heath, J. R., Kondratenko, M., Perepichka, D. F., Arseneault, K., Pezolet, M. & Bryce, M. R. (2005) *Chem. Eur. J.* 11, 2914-2922.

60. McCreery, R. L. (2004) *Chem. Mater.* 16, 4477-4496

61. Metzger, R. M. (2003) *Chem. Rev.* 103, 3803-3834.

62. Metzger, R. M., Baldwin, J. W., Shumate, W. J., Peterson, I. R., Mani, P., Mankey, G. J., Morris, T., Szulczewski, G., Bosi, S., Prato, M., Comito, A. & Rubin, Y. (2003) *J. Phys. Chem. B* 107, 1021-1027.

63. Ashwell, G. J., Urasinska, B. & Tyrrell, W. D. (2006) *Phys. Chem. Chem. Phys.* 8, 3314-3319.

64. McCreery, R., Dieringer, J., Solak, A. O., Snyder, B., Nowak, A. M., McGovern, W. R. & DuVall, S. (2003) *J. Am. Chem. Soc.* 125, 10748-10758.

65. Taylor, J., Brandbyge, M. & Stokbro, K. (2002) *Phys. Rev. Lett.* 89.

66. Asakawa, M., Higuchi, M., Mattersteig, G., Nakamura, T., Pease, A. R., Raymo, F. M., Shimizu, T. & Stoddart, J. F. (2000) *Adv. Mat.* 12, 1099-1102.

67. Ashton, P. R., Horn, T., Menzer, S., Preece, J. A., Spencer, N., Stoddart, J. F. & Williams, D. J. (1997) *Synthesis-Stuttgart*, 480-488.

68. Brown, C. L., Jonas, U., Preece, J. A., Ringsdorf, H., Seitz, M. & Stoddart, J. F. (2000) *Langmuir* 16, 1924-1930.

69. Tseng, H. R., Wu, D. M., Fang, N. X. L., Zhang, X. & Stoddart, J. F. (2004) *Chemphyschem* 5, 111-116.

70. Lu, T. B., Zhang, L., Gokel, G. W. & Kaifer, A. E. (1993) *J. Am. Chem. Soc.* 115, 2542-2543.

71. Asakawa, M., Ashton, P. R., Balzani, V., Brown, C. L., Credi, A., Matthews, O. A., Newton, S. P., Raymo, F. M., Shipway, A. N., Spencer, N., Quick, A., Stoddart, J. F., White, A. J. P. & Williams, D. J. (1999) *Chem. Eur. J.* 5, 860-875.

72. Saha, S., Johansson, E., Flood, A. H., Tseng, H. R., Zink, J. I. & Stoddart, J. F. (2005) *Chem. Eur. J.* 11, 6846-6858.

73. Chia, S. Y., Cao, J. G., Stoddart, J. F. & Zink, J. I. (2001) *Angew. Chem. Int. Ed.* 40, 2447-2451.

74. Katz, E., Baron, R., Willner, I., Richke, N. & Levine, R. D. (2005) *Chemphyschem* 6, 2179-21789.

75. Katz, E., Lioubashevsky, O. & Willner, I. (2004) *J. Am. Chem. Soc.* 126, 15520-15532.

76. Long, B., Nikitin, K. & Fitzmaurice, D. (2003) *J. Am. Chem. Soc.* 125, 5152-5160.

77. Long, B., Nikitin, K. & Fitzmaurice, D. (2003) *J. Am. Chem. Soc.* 125, 15490-15498.

78. Nikitin, K. & Fitzmaurice, D. (2005) *J. Am. Chem. Soc.* 127, 8067-8076.

79. Flood, A. H., Peters, A. J., Vignon, S. A., Steuerman, D. W., Tseng, H. R., Kang, S., Heath, J. R. & Stoddart, J. F. (2004) *Chem. Eur. J.* 10, 6558-6564.

80. Choi, J. W., Flood, A. H., Steuerman, D. W., Nygaard, S., Braunschweig, A. B., Moonen, N. N. P., Laursen, B. W., Luo, Y., DeIonno, E., Peters, A. J., Jeppesen, J. O., Xu, K., Stoddart, J. F. & Heath, J. R. (2006) *Chem. Eur. J.* 12, 261-279.

81. Collier, C. P., Jeppesen, J. O., Luo, Y., Perkins, J., Wong, E. W., Heath, J. R. & Stoddart, J. F. (2001) *J. Am. Chem. Soc.* 123, 12632-12641.

82. Diehl, M. R., Steuerman, D. W., Tseng, H. R., Vignon, S. A., Star, A., Celestre, P. C., Stoddart, J. F. & Heath, J. R. (2003) *Chemphyschem* 4, 1335-1339.

83. Laursen, B. W., Nygaard, S., Jeppesen, J. O. & Stoddart, J. F. (2004) *Org. Lett.* 6, 4167-4170.

84. Green, J. E., Choi, J. W., Boukai, A., Bunimovich, Y., Johnston-Halperin, E., DeIonno, E., Luo, Y., Sheriff, B. A., Xu, K., Shin, Y. S., Tseng, H. R., Stoddart, J. F. & Heath, J. R. (2007) *Nature* 445, 414-417.

85. Tseng, H. R., Vignon, S. A., Celestre, P. C., Perkins, J., Jeppesen, J. O., Di Fabio, A., Ballardini, R., Gandolfi, M. T., Venturi, M., Balzani, V. & Stoddart, J. F. (2004) *Chem. Eur. J.* 10, 155-172.

86. Riehn, R., Lu, M. C., Wang, Y. M., Lim, S. F., Cox, E. C. & Austin, R. H. (2005) *Proc. Nat. Acad. Sci.* 102, 10012-10016.

87. Karnik, R., Fan, R., Yue, M., Li, D. Y., Yang, P. D. & Majumdar, A. (2005) *Nano Lett.* 5, 943-948.

88. Stein, D., Kruithof, M. & Dekker, C. (2004) *Phys. Rev. Lett.* 93, 035901.

89. Karnik, R., Castelino, K., Fan, R., Yang, P. & Majumdar, A. (2005) *Nano Lett.* 5, 1638-1642.

90. Hinds, B. J., Chopra, N., Rantell, T., Andrew, R., Gavalas, V. & Bachas, L. G. (2005) *Science* 303, 62-65.

91. Holt, J. K., Park, H. K., Wang, Y., Stadermann, M., Artyikhin, A. B., Grigoropuoulos, S. P., Noy, A. & Bakajin, O. (2006) *Science* 312, 1034-1037.

92. Majumdar, M., Chopra, N., Andrew, R. & Hinds, B. J. (2005) *Nature* 438, 44-44.